A 7T 8 channel transmit-receive dipole array for head imaging: dipole element and coil evaluation

Gang Chen[1], Martijn Cloos[1], Daniel Sodickson[1], and Graham Wiggins[1]

[1]The Bernard and Irene Schwartz Center for Biomedical Imaging, Department of Radiology, New York University School of Medicine, New York, NY, United States

Target audience: Radiofrequency (RF) engineers, anyone interested in high field RF coils, parallel transmit or high field brain imaging.

Introduction: Electric dipole antennas are seeing increasing use for 7T MR imaging[1-3]. They differ from conventional surface coil loops in many ways. With 8 elements surrounding a body sized tissue equivalent phantom and array of dipole antennas can achieve higher central SNR than an array of loops, while simultaneously having greater coverage along Z^4. Most 7T head coils today rely on birdcage or TEM volume coils for transmit, or arrays of loops. Signal dropout in inferior brain regions such as the cerebellum and brain stem is a common problem. We describe here a dipole array for 7T head imaging designed for extended coverage and evaluate its performance in phantom and volunteer imaging.

The simplest form of electric dipole antenna is a self-resonant straight conductor whose length is $\lambda/2$ in free space. When placed close to the head the self-resonant length reduces to about 44 cm, which is long enough to interfere with the shoulders if the dipoles are centered on the brain. We therefore evaluated a range of shortened dipole element designs in simulations before choosing one for array construction.

Figure 1: Original dipole and 3 shortened dipoles setup in Simulation

a) Simulation Setup   b) Constructed Coil

Methods: FDTD simulations were performed with Microwave Studio (CST, Darmstadt, Germany). Various dipole element designs with 7mm conductor width were simulated 2 cm above a 38x25x50 cm rectangular phantom with $\varepsilon_r = 59$ and $\sigma = 0.77$. The simple dipole is self resonant at 297.2 MHz when it is 46.6 cm long. Various strategies were employed to shorten the length of dipoles to 32 cm while maintaining resonance at 297.2 MHz, including meanders at the ends of the dipoles, lumped element inductors by the feed point and meanders at intervals along the length of the dipole (fractionated dipole)[3] (Fig. 1). The 8 channel dipole array was modeled on a 27.9 cm diameter cylinder (Fig. 2), loaded with a head shaped phantom with uniform electrical properties ($\varepsilon_r = 52$, $\sigma = 0.56$). Dipole elements 32 cm in length with meanders at each end were arranged similarly to the rungs on a birdcage. All elements were tuned and matched in the simulation.

An 8 channel array was constructed based closely on the simulated design. Each element was matched using a parallel capacitor and a $\lambda/2$ balun, and 2 cable traps were used in the coaxes feeding each antenna. The coil was interfaced to a 7T scanner with 8 channel parallel transmit (Siemens, Erlangen Germany) using an in-house built transmit-receive interface. Data were obtained on a gel phantom with the same shape and properties used in the simulations and with a human volunteer after establishing safe power limits on the gel phantom using MR thermometry. Phases to the elements were chosen to create constructive interference at the center of the object. B_1^+ maps were obtained with a turbo-FLASH sequence with preparation pulse [5], and SNR maps were generated based on GRE measurements obtained with RF excitation and without (TR/TE/BW=200/4.1/300, FOV=220mm, Matrix=256, Slice = 3 mm). The dipole array was also compared to the transmit birdcage of a commercially available 7T head coil (Nova Medical. Wilmington, MA)

Figure 4: 8 channel meander ends dipole array simulation setup and constructed coil

Results: In the simulation, 10g peak local SAR for original dipole, inductor shortened dipole, fractionated dipole and meander ends dipole were 0.58, 0.91, 0.84 and 0.65 w/kg respectively. B_1^+ maps normalized by the square root of 10g peak local SAR are shown in Figure 3. Figure 4 shows B_1^+ profiles along the center line for each dipole design.

For the constructed 8 channel dipole array, the average decoupling between adjacent elements were -10 dB, and S11 of -20 dB or better was achieved on all elements. B_1^+ maps obtained from simulation and experiment are shown in Figure 5, and also B_1^+ maps from the Nova Medical volume coil. The excitation patterns in simulation and experiment are similar, and the extended coverage in the neck compared to the Nova coil is evident. To achieve a 90 degree flip angle in the center of the object with a 500 µs hard pulse required 173 volts on the phantom (61 v per channel) and 283 volts in the volunteer with the dipole array. For the Nova coil the values were 187 and 235 volts respectively. SNR plots of root sum of squares reconstruction in the head shaped gel phantom and in volunteer for the dipole array and Nova Medical coil are shown in Figure 6.

Figure 3: coronal view B_1^+ of 4 dipole designs in simulation.

Figure 4: B_1^+ profile for 4 dipoles along z direction

Discussion Figure 3 shows that Inductor shortened and fractionated dipole has high B_1^+ intensity in the center, but suffers from fast drop off towards the ends of the antenna, which can also be seen in Figure 4. The dipole with meander ends has larger coverage and smaller peak local SAR, and therefore is more favorable than the other 2 designs. B_1^+ efficiency and central SNR were similar for the dipole array and Nova coil in the phantom, but the dipole array compared less favorably in the volunteer scan. We attribute this to excessive loading of the coil by the shoulders, a by-product of the design criterion to provide extended coverage.

Conclusions: The dipole array extends coverage into the cerebellum and C-spine, but at the cost of lower B_1^+ efficiency. This suggests that the dipole element has to be further shortened. Shielding may also be applied to prevent loading of the array by the shoulders and torso.

References: [1] Raaijmakers AJE. Magn Reson Med 2011 66(5):1488-97 [2] Ozerdem C. ISMRM 2012 p2641 [3] Raaijmakers AJE. ISMRM 2013 p4382 [4] Wiggins GC. ISMRM 2012 p541. [5] Klose U, Med. Phys. 19 (4), 1992
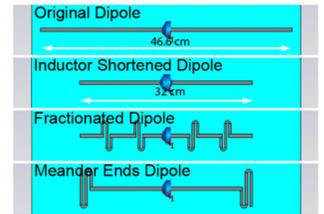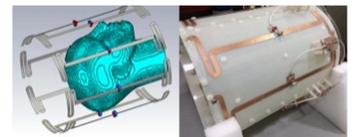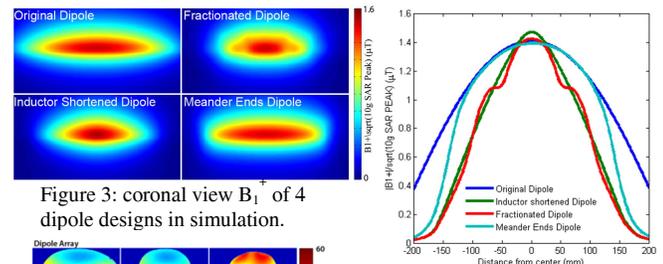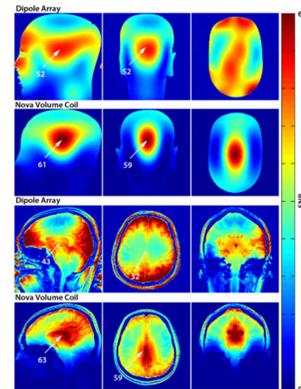
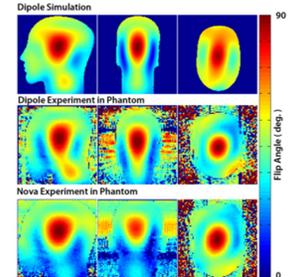Figure 6: SNR plots of root sum of squares reconstruction for the 2 coils in head shaped gel phantom and in volunteer

Figure 5: B_1^+ comparison for the 2 coils